https://doi.org/ 10.33472/AFJBS.6.9.2024.3529-3543

African Journal of Biological Sciences

Journal homepage: http://www.afjbs.com

Research Paper Open Access

Effect of Deposition Cycles on Structural and Electrochemical Properties of Fe_2O_3 Thin Film Electrodes Synthesized by SILAR Technique for Supercapacitor Applications

Sanjaykumar S. Pujari[1], Ashruba Waghmare, Rushikesh. G. Bobade [2], Revanappa. C. Ambare [2,*] Balkrishna. J. Lokhande [1*],

[1] Lab of Electrochemical Studies, School of Physical Sciences, PSAH Solapur University, Solapur, Maharashtra, India.

[2] Department of Physics, KMC, College, Khopoli-410203, Raigad (Affiliated to University of Mumbai), Maharashtra, India.

[*]**Corresponding author: Dr. B. J. Lokhande, E-mail:** bjlokhande@yahoo.com

Dr. R.C. Ambare, E-mail: revanambare@gmail.com,

Article History

Volume 6,Issue 9, 2024

Received: 28 Apr 2024

Accepted : 10 May 2024

doi: 10.33472/AFJBS.6.9.2024.3529-3543

Abstract

A promising thin film electrode material, ferric oxide (Fe_2O_3), was synthesized using the successive ionic layer adsorption and reaction (SILAR) technique for application in supercapacitors. Characterization of the Fe_2O_3 thin films was carried out using various analytical tools, including X-ray diffraction (XRD), field emission scanning electron microscopy (FE-SEM), and energy dispersive X-ray analysis (EDAX). The electrochemical performance of the thin films was assessed through cyclic voltammetry (CV), galvanostatic charge-discharge (GCD) measurements, and electrochemical impedance spectroscopy (EIS). The highest specific capacitance (Cs) recorded was 596 F/g at a scan rate of 5 mV/s in a 1 M KOH electrolyte. Additionally, the maximum energy density and power density obtained were 25.4 Wh/kg and 0.5 W/kg, respectively, at a current density of 1 mA/cm² in 1 M KOH. The internal resistance of the Fe_2O_3 thin film was found to be approximately 1.1 Ω. These results demonstrate that Fe_2O_3 is found suitable as a high-performance thin film electrode material for supercapacitors.

Keywords: Fe_2O_3, Nanomaterials, SILAR, Supercapacitor application, Thin film.

1. Introduction

Iron oxide (Fe_2O_3), a transition metal oxide, has garnered significant attention in recent years due to its unique physicochemical properties and wide range of applications. These include uses in photocatalysis, sensors, lithium-ion batteries, magnetic data storage, and biomedical applications. The versatility and functionality of Fe_2O_3 are largely attributable to its polymorphic forms, notably hematite (α-Fe_2O_3), magnetite (Fe_3O_4), and maghemite (γ-Fe_2O_3) [1][2]. Among these, hematite is particularly valued for its stability, environmental benignity, and cost-effectiveness, making it a compelling material for various technological applications. The synthesis of Fe_2O_3 has been achieved through a plethora of methods, including sol-gel processes, hydrothermal synthesis, co-precipitation, and chemical vapor deposition. However, these methods often entail high temperatures, prolonged reaction times, and intricate processing conditions. In contrast, the Successive Ionic Layer Adsorption and Reaction (SILAR) method stands out as a straightforward, low-temperature, and cost-effective technique for producing high-quality thin films of Fe_2O_3. The SILAR method, developed as an extension of the chemical bath deposition technique, involves the alternate dipping of a substrate into separate cationic and anionic precursor solutions, allowing for controlled layer-by-layer growth of the material [3][4].

The SILAR method offers several advantages: it allows precise control over the film thickness and composition by adjusting the number of deposition cycles, and it does not require sophisticated equipment or high vacuum conditions, which makes it accessible and scalable. Additionally, the process parameters, such as the concentration of precursor solutions, immersion times, and washing steps, can be fine-tuned to optimize the properties of the resulting Fe_2O_3 films. In this study, we have synthesized Fe_2O_3 thin films using the SILAR method with varying numbers of deposition cycles to investigate the effect of cycle variation on the structural, morphological, and optical properties of the films [5][6]. The deposition cycle is a critical parameter in the SILAR process, as it directly influences the thickness, crystallinity, and surface roughness of the films. By systematically varying the number of cycles, we aim to gain insights into the growth mechanisms of Fe_2O_3 films and their potential impact on performance in practical applications [4] [5][6][7][8].

In this research understanding the relationship between the deposition cycle number and the resulting properties of Fe_2O_3 films is crucial for optimizing their performance in supercapacitor applications. This research not only provides a detailed investigation of the synthesis and properties of Fe_2O_3 thin films prepared by the SILAR method but also contributes to the broader understanding of how deposition parameters can be leveraged to tailor material properties for specific applications. The findings from this study could pave the way for the development of advanced Fe_2O_3-based materials with enhanced performance in energy conversion, environmental remediation, and supercapacitor applications.

2. Experimental

2.1 Materials

Ferric nitrate formula [$Fe(NO_3)_3$] (99% extra pure). sodium hydroxide pallets [NaOH] (98% extra pure), hydrochloric acid [HCl], and acetone. All chemicals purchased from SDFCL chemical Ltd. All chemicals were used without using extra purification. Stainless steel (SS) was used as a conducting working electrode.

2.2 Electrode preparation

Stainless steel (SS) was selected as a cost-effective and versatile conducting substrate for the supercapacitor due to its stability in neutral, alkaline, and acidic aqueous electrolytes. The SS working electrodes were polished using 1200-grade abrasive paper to achieve a refined surface. Following this, the electrodes underwent ultrasonic cleaning in a 10% HCl solution for 30-40 minutes to ensure thorough surface preparation. The SS substrates were then meticulously rinsed with acetone and distilled water to eliminate any remaining contaminants [9].

2.3 Synthesis of Fe_2O_3 electrode

The Fe2O3 thin films were synthesized using the SILAR method with varying cycles to investigate their structural and optical properties. The deposition process involved a four-beaker setup: the 0.2 M [$Fe(NO_3)_3$] solution as the cation source, two distilled water beakers for rinsing, and the 0.2 M NaOH solution as the anion source. Each SILAR cycle consisted of immersing the SS substrate in the [$Fe(NO_3)_3$] solution for 30 seconds, rinsing in distilled water (DW) for 10 seconds, immersing in the NaOH solution for 30 seconds, and rinsing again in distilled water for 10 seconds. The cycle numbers were varied as 25, 50, and 75, and deposited sample were designated as CF1, CF2, and CF3, respectively. Post-deposition, the films were calcined at 350°C for 2 hours to convert $Fe(OH)_3$ to Fe_2O_3. This systematic variation in the number of deposition cycles aimed to tailor the film properties for potential applications [1][2][9].

2.4 Characterization details

The crystal structure, and plane orientations were determined using an XRD spectrum on a Rigaku D/max 2550 V^{b+}/PC 18 kW with Cu K, = 1.5406 diffractometer. Microstructure photographs are obtained with a Hitachi S-4800, 15 kV FE-SEM. The Holmark HO-IAD-CAN-01 device instrument was used to gauge the contact angle of a deposited electrode. The weight difference approach was utilized to calculate the weight of the depositing material using a 1 $x10^{-6}$ high precision analytical microbalance (Tapson's-100 TS). Hitachi's (H-7650) TEM. LaB6 electron source voltage used to accelerate: 80 to 120 kV, 0.36 for point resolution and 0.24 for line resolution in nanometres Magnification: HR mode: ×4000 – ×600000, HC mode: x200–x200000, Field rotation was 900 (150 steps) for an ×1000 – ×40000 magnification range. Three electrode cells of a Fe_2O_3 film electrode were evaluated for their electrochemical properties using a potentiostat (HCH 600D SPL. electrochemical analyzer/workstation). In the supercapacitive inquiry, saturated Ag/AgCl was used as a reference electrode, and platinum wire was used as a counter electrode during the CV of the generated substrate (size 1.5 cm^2) in 1 M KOH. The collected CV plots were used to determine the Cs in F/g. GCD was used to study charge-discharge at varying current densities to determine SE, SP and ɳ. A multi-frequency EIS test was carried out utilizing an AC signal to assess a supercapacitor cell's internal resistance in the frequency range of 1 mHz to 1 MHz.

2.5 Electrochemical measurements

The electrochemical properties of the individual electrodes were evaluated using the HCH 600D SPL electrochemical workstation. The working electrodes, composed of Fe_2O_3, were tested in a 1 M KOH solution, with an Ag/AgCl reference electrode and a platinum (Pt) wire serving as the counter electrode. The electrodes underwent examination using cyclic voltammetry (CV) and chronopotentiometry (CP) within a potential range of -1.37 to 0.36 V.

Electrochemical impedance spectroscopy (EIS) analysis was performed over a frequency range from 1 mHz to 1 MHz with an A.C. amplitude of 5 mV. The specific capacitance (Cs) in F/g of the electrodes was determined from the CV curves according to the method described [9]. Additionally, the specific energy (SE) in Wh/kg and specific power (SP) in kW/kg were calculated from the CP plots using the same reference [9][10]:

$$SC = \frac{1}{mv\,(v_f - v_i)} \int_{v_i}^{v_f} I\,(V)\,dv \qquad (1)$$

$$SE = \frac{V \times I_d \times t_d}{m} \qquad (2)$$

$$SP = \frac{V \times I_d}{m} \qquad (3)$$

Where (V_f - V_i) potential window, 'm' active mass on electrode, 'V' sweeping rate in mV/s, 'I (V)' current in mA, 'I_d' discharging current, and 'td' discharging time in sec.

3. Results and discussion

3.1 XRD analysis

The Fe_2O_3 nanostructures deposited at 632 K were visible in the XRD pattern in **Fig. 1**. The fact that the peaks are oriented suggests that barium oxide was forming at this temperature. The typical arrangement of the hexagonal phase of Fe_2O_3 (JCPDS card no. 33-0664) have well matched by the increased prominence and clarity of the diffraction peaks. It clearly exhibits the peaks at angles 43.4°, 44.5°, 50.4°, 74.6°, and 82.4°, corresponds to (202), (024), (116), (220), and (015) planes, similar results reported by Xia *et al* [11]. There were no more phase peaks seen, proving that the hydroxide which was entirely converted into Fe_2O_3. Scherrer's formula [10][12] was used to determine that the average particle size was approximately 58.1 nm, 44.7 nm, and 64.9 nm of CF1, CF2, and CF3 electrode respectively shown in **Table 1**.

$$D = \frac{K\lambda}{\beta\, cos\theta} \qquad (1)$$

Where, 'K' constant (0.9), 'λ' wavelength of X-ray, 'β' full-width half maximum (FWHM), and 'θ' Braggs angle.

The micro strain was determined by using the below relation.

$$\varepsilon = \frac{\beta}{4\tan\theta} \qquad (2)$$

The calculated value of the micro strain [10] of Fe_2O_3 was 0.0264, 0.0422, and 0.0132 of CF1, CF2, and CF3 respectively shown in **Table 1**.

The dislocation density was determined by using the below relation.

$$\delta = \frac{1}{D^2} \qquad (3)$$

The calculated value of the dislocation density [12] of Fe_2O_3 was 5.39, 7.67, 3.54, of CF1, CF2, and CF3 respectively shown in **Table 1**.

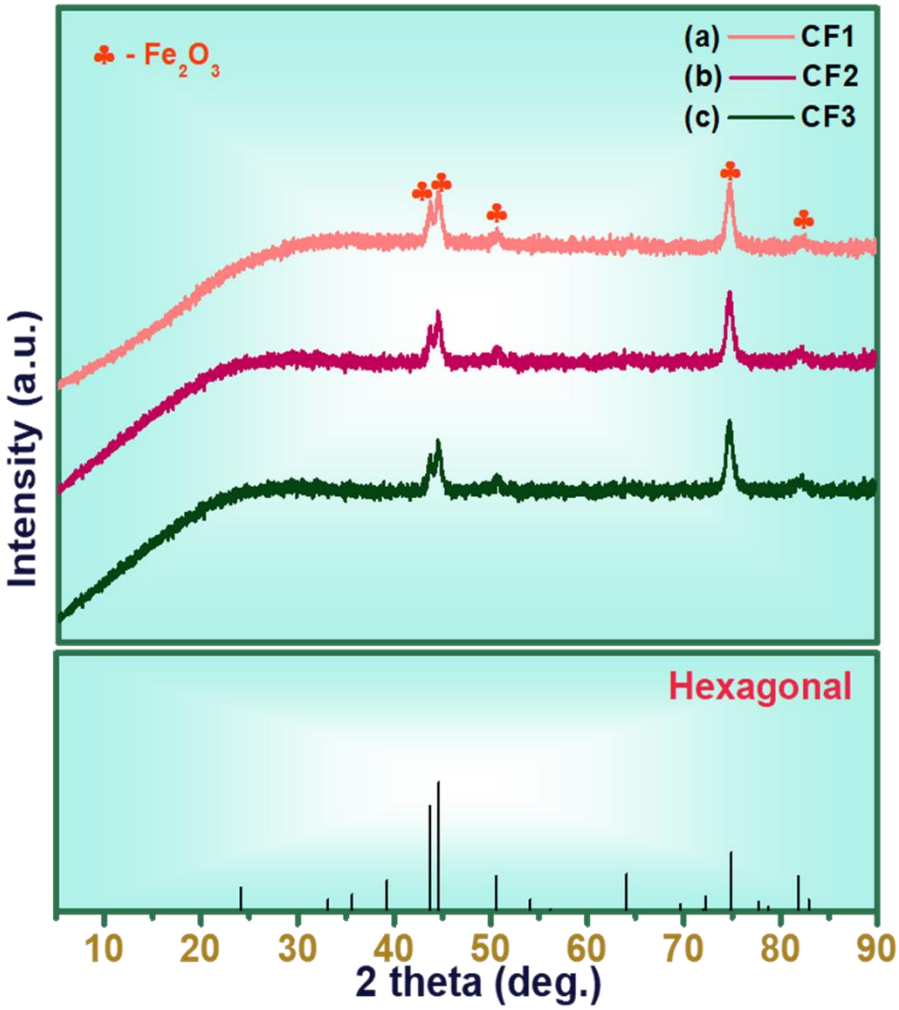

Fig 1: XRD plots of sample **(a)** CF1, **(b)** CF2, and **(c)** CF3.

Table 1: Structural variation of CF1, CF2, and CF3 electrode in terms of crystalline size, micro strain, and dislocation density.

Sample code	**Crystallite size (D) (nm)**	**Micro strain (ε) (10^{-3})**	**Dislocation density (δ) (× 10^{15}) lines m^{-2}**
CF1	58.1	0.0264	5.39
CF2	44.7	0.0422	7.67
CF3	64.9	0.0132	3.54

3.2 Morphological analysis

3.2.1 FE-SEM and EDAX study

Fig 2 (a-d) shows the morphological characteristics of Fe_2O_3 thin films synthesized via the SILAR method, with varying cycle, were investigated using field emission scanning electron microscopy (FE-SEM). FE-SEM images at magnifications of 10 μm and 1 μm revealed a consistent small grain-like morphology across all samples. At the higher magnification of 1 μm, the images clearly displayed well-defined, small grain-like structures uniformly distributed across the surface of the thin films similar results reported by Maile *et al* [1]. Notably, the 1 μm magnification images exhibited well-defined grain structures. The grain size analysis showed that the sample CF2 had an average grain size of 48.4 nm, while CF3 displayed larger grains with an average size of 65.9 nm. These observations indicate that an increase in the number of deposition cycles results in larger grain sizes, which could influence the electrochemical properties and performance of the Fe_2O_3 thin films. **Fig. 3 (a)** shows the existence of chemical elements such as Fe, and O that were confirmed for Fe2O3. It was confirmed that Fe_2O_3 Nanomaterials had formed by the substantial compositions analysis findings obtained by EDAX. In the spectrum, the quantity in weight % of Fe, and O were 94.91%, and 5.09% respectively. and atomic% of Fe, and O were 84.24%, and 15.76% respectively. The Elemental mapping analysis of the CF2 sample is shown in **Fig. 3 (b-d)**. The image shows that all of the elements Fe, and O are present. The presence of chemical elements and their compositional ratio were analyzed using EDAX mapping.

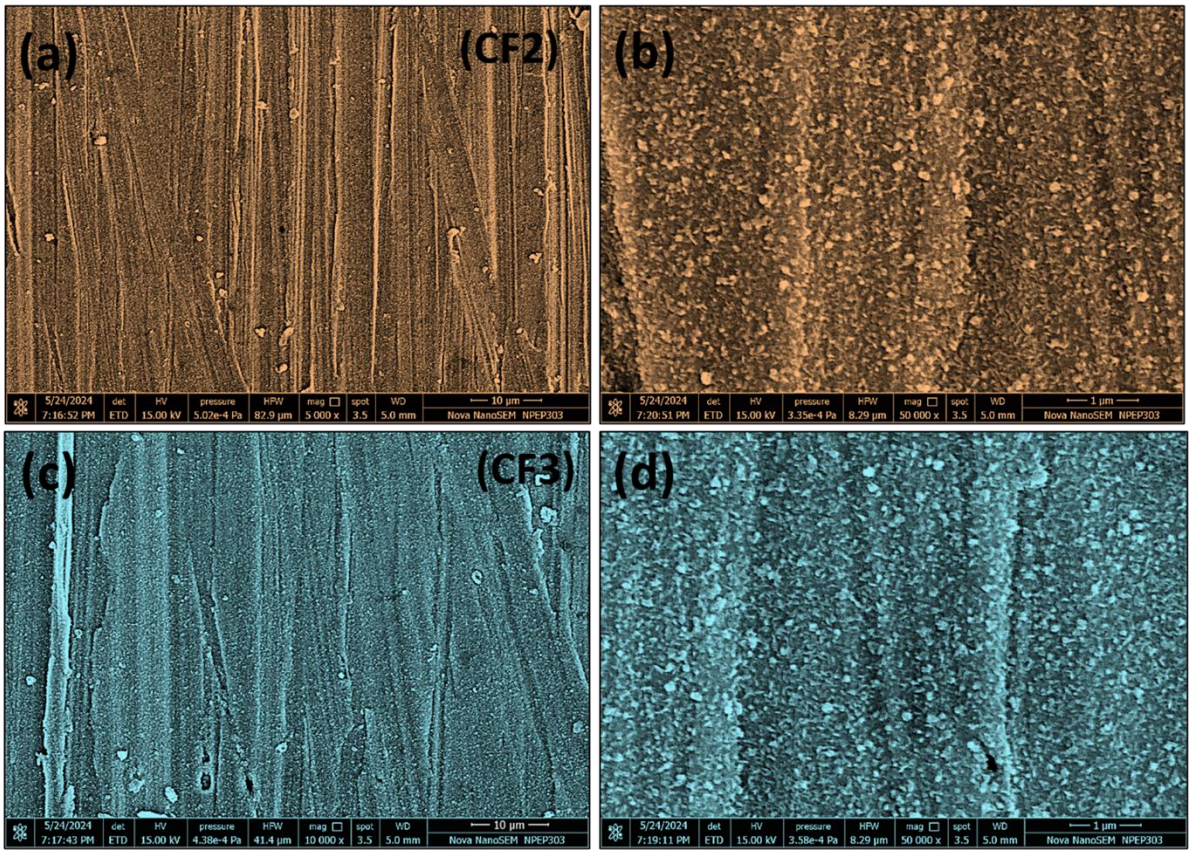

Fig 2: FE-SEM images of sample **(a-b)** CF2, **(c-d)** CF3.

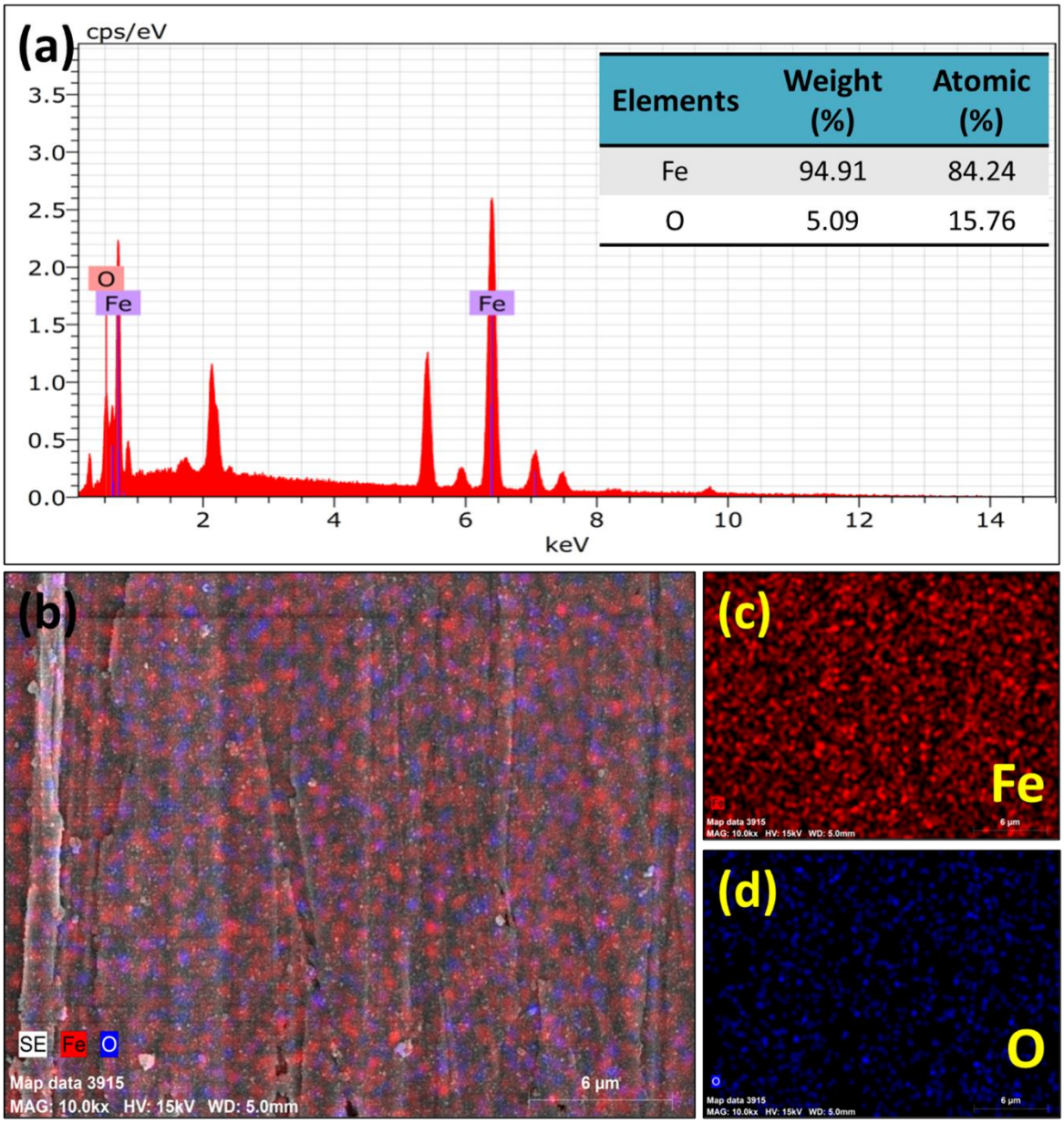

Fig 3: (a) EDAX spectrum with percentage of chemical elements present in CF2 electrode, **(b)** The EDAX mapping image of CF2 electrode, and **(c-d)** Elemental mapping images showing the individual distribution of Fe, and O.

3.2.2 Wettability study

The wettability of the Fe_2O_3 thin films synthesized using the SILAR method with varying cycle numbers was assessed through contact angle measurements. The contact angles for the samples CF1, CF2, and CF3 were found to be 112°, 66.6°, and 93.4°, respectively shows in **Fig. 4**. These values indicate significant differences in surface hydrophilicity and hydrophobicity among the samples. Specifically, CF1 exhibited the highest contact angle, suggesting a more hydrophobic surface, whereas CF2 displayed the lowest contact angle, indicating a highly hydrophilic surface. CF3, with an intermediate contact angle, demonstrated moderate wettability. These variations in contact angles can be attributed to the differences in surface morphology and grain size induced by the different numbers of SILAR

cycles, which influence the surface energy and, consequently, the wettability properties of the Fe_2O_3 thin films.

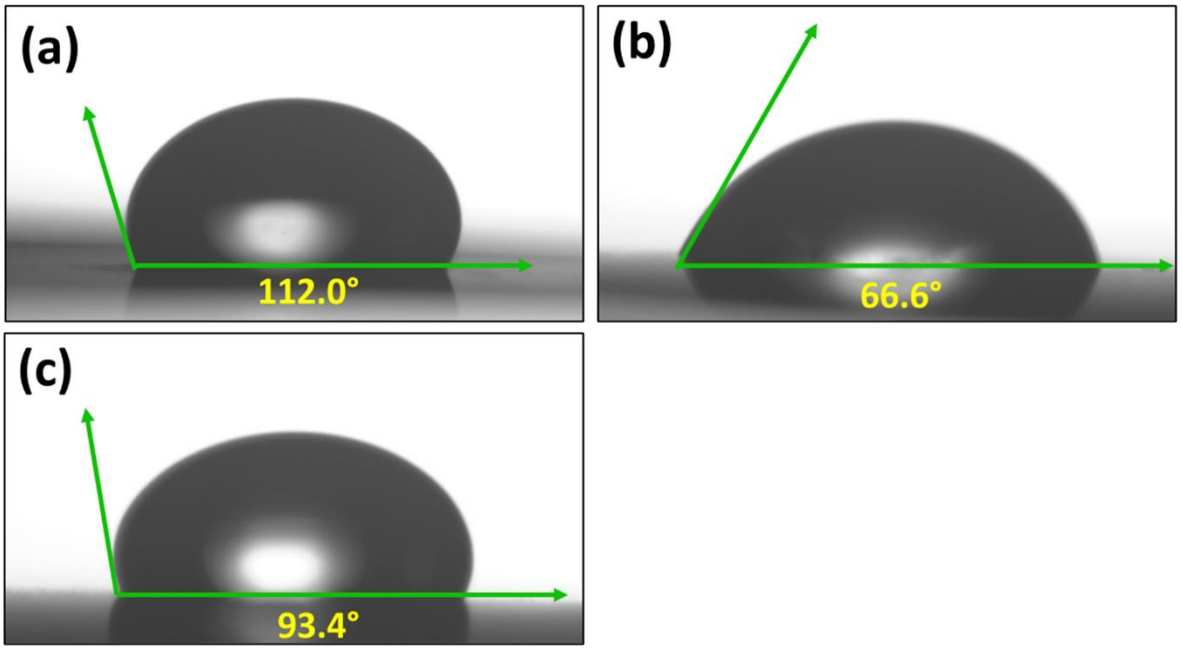

Fig 4: Contact angle images of sample **(a)** CF1**, (b)** CF2**, (c)** CF3**.**

3.3 Electrochemical supercapacitor analysis

3.3.1 Cyclic voltammetry study

The cyclic voltammetry (CV) analysis of Fe_2O_3 thin films synthesized via the SILAR method with varying cycle numbers, revealed significant insights into their electrochemical performance shows in **Fig 5 (a)**. Conducted in a 1 M KOH electrolyte with a potential window of -1.4 to 0 V versus Ag/AgCl at a scan rate of 5 mV/s, the specific capacitance values for CF1, CF2, and CF3 were determined to be 228.3 F/g, 596 F/g, and 535.5 F/g, respectively shown in **Fig 5 (b)**. **Table 2** shows the variation of Cs in F/g at scan rate of 5 mV/s for different electrode (CF1, CF2, CF3). Morphological analysis indicated that all samples exhibited a small grain-like morphology, with CF2 having the smallest grain size and the highest crystallinity. Additionally, CF2 displayed a lower wettability angle compared to the other samples, suggesting enhanced surface hydrophilicity. The superior specific capacitance of CF2 can be attributed to its smaller grain size and higher crystallinity, which provide a greater active surface area and more efficient charge storage capability [13]. These findings underscore the significant impact of cycle variation on the electrochemical properties of Fe2O3 thin films, highlighting CF2 as a particularly promising material for high-performance supercapacitors.

Fig 5 (c) shows the cyclic voltammetry (CV) study of the optimized Fe2O3 thin film electrode (CF2), was conducted at varying scan rates of 5, 10, 20, 50, and 100 mV/s in a 1 M KOH electrolyte with a potential window of -1.4 to 0 V versus Ag/AgCl. The specific capacitance values obtained for CF2 were 596 F/g at 5 mV/s, 551.8 F/g at 10 mV/s, 490.8 F/g at 20 mV/s, and 446.6 F/g at both 50 and 100 mV/s shown in **Fig 5 (d)**. **Table 3** shows the **v**ariation of Cs in F/g at different scan rate of CF2 electrode The decrease in specific capacitance with increasing scan rates indicates that at lower scan rates, the electrolyte ions

have sufficient time to penetrate the electrode material fully, resulting in higher capacitance. In contrast, at higher scan rates, the diffusion of ions is limited, leading to lower capacitance values [14]. These results demonstrate the excellent capacitive performance of the CF2 electrode, particularly at lower scan rates, underscoring its potential for application in high-performance supercapacitors. **Table 4** shows the comparison of electrochemical characteristics of Fe_2O_3 with other reported Fe_2O_3-based thin film in aqueous electrolyte.

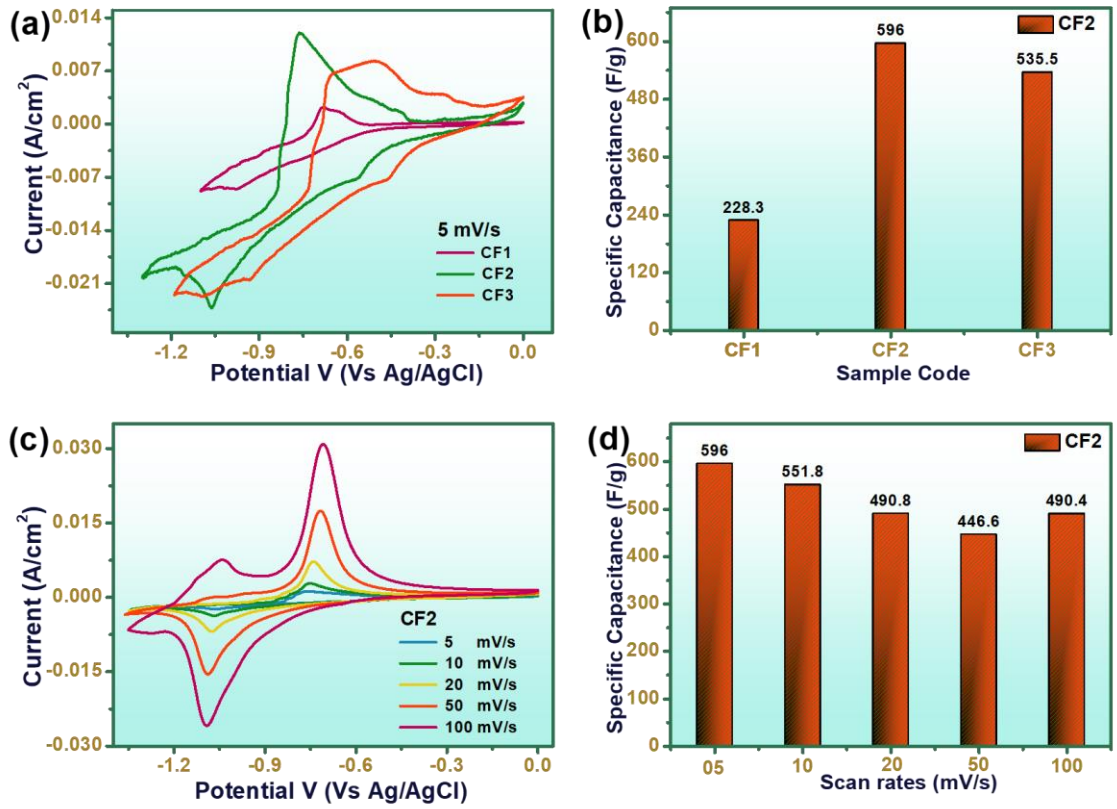

Fig 5: (a) CV plots of electrode CF1, CF2, and CF3, **(b)** specific capacitance vs sample code at 5 mV/s, **(c)** CV plots electrode CF2 at scan rate of 5 -100 mV/s in 1 M KOH, **(d)** specific capacitance vs scan rate in mV/s of electrode CF2.

Table 2: Variation of Cs in F/g at scan rate of 5 mV/s for different electrode (CF1, CF2, CF3).

Sample code	**Cs in F/g at scan rate of 5 mV/s**
CF1	228.3
CF2	596
CF3	535.5

Table 3: Variation of Cs in F/g at different scan rate of CF2 electrode.

Scan rate in mV/s	Cs in F/g
05	596
10	551.8
20	490.8
50	446.6
100	490.4

Table 4: Comparison of electrochemical characteristics of Fe_2O_3 with other reported Fe_2O_3-based thin film in aqueous electrolyte.

Material	**Synthesis method**	**Electrolyte**	**Potential window**	**Cs (F/g)**	**Ref.**
Fe_2O_3	Sol-gel	0.5M Na2SO3	-0.8 - 0 V vs SCE	300	[4]
Fe_2O_3	Electrospinning	1M LiOH	-0.1 - 0.9 Vvs Ag/AgCl	256	[5]
Fe_2O_3	Anodization	1 M Li2SO4	-0.8 - 0 V vs SCE	138	[6]
Fe_2O_3	Solvothermal	1 M KOH	-0.1 - 0.4 V vs Ag/AgCl	145	[7]
Fe_2O_3	Wet chemical	1 M H3PO4	- 0.1 - 0.9 V vs Ag/AgCl	308	[8]
Fe_2O_3	SILAR	1 M KOH	-1.4 – 0 V vs Ag/AgCl	596	Recent Work

3.3.2 Chronopotentiometry study

The galvanostatic charge-discharge (GCD) analysis of Fe_2O_3 thin films synthesized by the SILAR method with cycle variations, revealed distinct electrochemical properties. The measurements were performed at a current density of 1 mA/cm² in a 1 M KOH electrolyte, with a potential window from -1.4 to 0 V versus Ag/AgCl shows in **Fig. 6 (a)**. The specific energy values for CF1, CF2, and CF3 were found to be 23.5 Wh/kg, 25.4 Wh/kg, and 14.1 Wh/kg, respectively. The specific power values were 0.3 kW/kg for CF1, 0.5 kW/kg for CF2, and 0.4 kW/kg for CF3. Correspondingly, the efficiency values were 35.3% for CF1, 65.3% for CF2, and 47.1% for CF3 shows in **Fig. 6 (b)**. Morphological studies showed that all samples exhibited a small grain-like structure, with CF2 having the smallest grain size and

highest crystallinity. This optimal morphology of CF2 contributed significantly to its superior GCD performance, indicating enhanced ion transport and charge storage capabilities. These findings suggest that CF2, with its optimized structural properties, holds great promise as a high-performance electrode material for supercapacitor applications. **Table 5** shows the specific energy, specific power, and efficiency of CF1, CF2, and CF3 electrode.

The particularly focusing on electrode CF2, revealed valuable insights into its electrochemical performance at varying current densities. GCD plots were obtained at current densities of 1, 2, 3, 4, and 5 mA/cm² in a 1 M KOH electrolyte, with a potential window from -1.4 to 0 V versus Ag/AgCl show in **Fig. 6 (c)**. At these current densities, CF2 exhibited specific energy values ranging from 25.4 Wh/kg at 1 mA/cm² to 3 Wh/kg at 5 mA/cm², indicating a gradual decrease in energy storage capacity with increasing current density. Conversely, specific power increased from 0.5 kW/kg at 1 mA/cm² to 2.5 kW/kg at 5 mA/cm², reflecting the electrode's ability to deliver higher power outputs at higher current densities show in **Fig. 6 (d)**. The corresponding efficiencies ranged from 65.3% to 27.3%, demonstrating the electrode's varying charge-discharge efficiency under different operating conditions. **Table 6** shows the SE, SP, and efficiency of CF2 electrode at different current density. These findings illustrate the importance of considering current density effects when assessing the electrochemical performance of Fe_2O_3 thin film electrodes for supercapacitor applications.

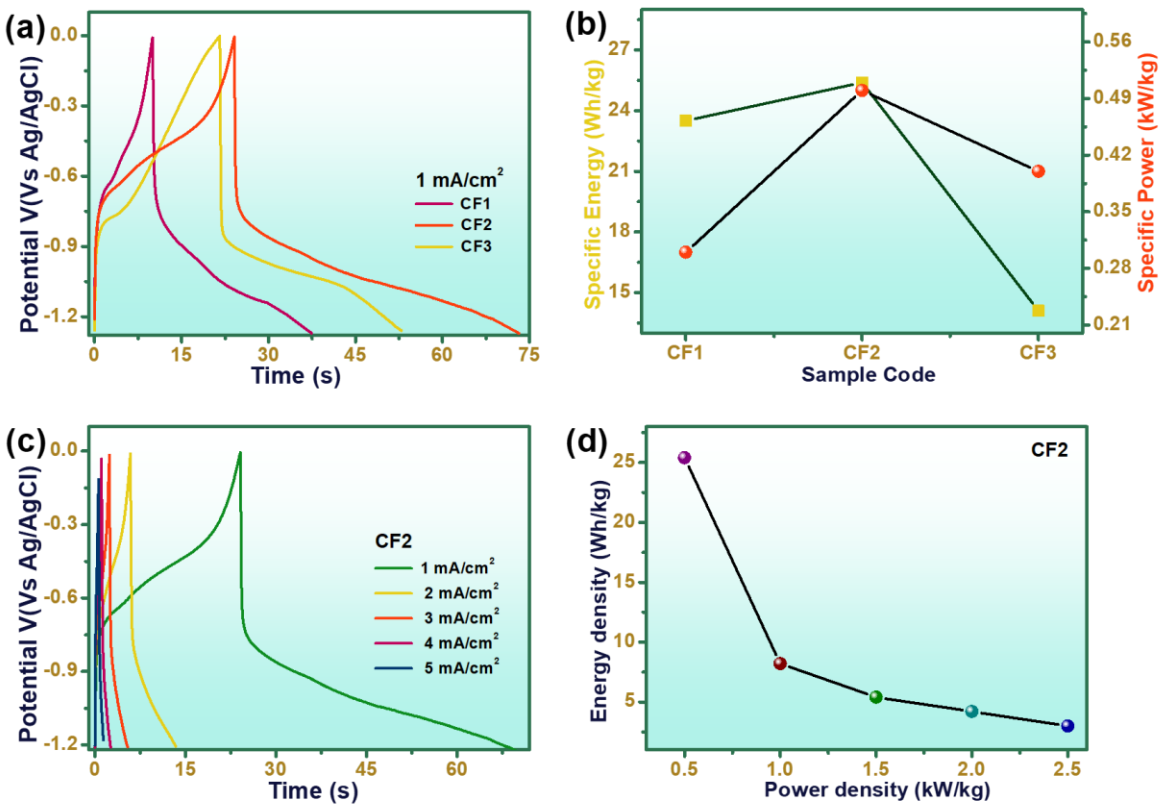

Fig 6: (a) The galvanostatic charge discharge curves of Fe_2O_3 at 1 mA/cm^2 in 1M KOH electrolyte, **(b)** Regon plots of different electrode CF1, CF2, and CF3, **(c)** The GCD curves of electrode CF2 at different current density from 1-5 mA/cm^2 in 1M KOH electrolyte, **(d)** Regon plot SE vs SP of electrode CF2.

Table 5: Specific energy, specific power, and efficiency of CF1, CF2, and CF3 electrode.

Sample code	Specific energy in (Wh/kg)	Specific power in (kW/kg)	Efficiency in (%)
CF1	23.5	0.3	35.3
CF2	25.4	0.5	65.3
CF3	14.1	0.4	47.1

Table 6: Specific energy, specific power, and efficiency of CF2 electrode at different current density.

Current density (mA)	Specific energy in (Wh/kg)	Specific power in (kW/kg)	Efficiency in (%)
1	25.4	0.5	65.3
2	8.2	1	69.6
3	5.4	1.5	60.6
4	4.2	2	40.3
5	3	2.5	27.3

3.3.3 Electrochemical impedance spectroscopy

Fig. 7 (a) depicts the Nyquist plot, which was used to examine the interior resistance and capacitive behavior of a working electrode CF1, CF2, and CF3 made of Fe_2O_3 using EIS extents in 1M KOH electrolyte, in the frequency range 100 Hz to 1 MHz. The **Fig. 7 (a)** was separated into three sections: a pseudocapacitive behaviour in the lower frequency zone and the charges transmission resistance (Rct) of the Faradaic reaction in the larger frequency region work together to produce a depressed half circle. The measured value of internal resistance (Ri) was 1.2 Ω, 1.1 Ω, 1.5 Ω of electrode CF1, CF2, and CF3 respectively. A knee frequency, or frequency where there was a departure from the semicircle, was shown to be the highest frequency at which capacitive performance predominates [13] [15].

The matched Nyquist graph of electrode CF2. A Nyquist curve for electrode CF2 attained via experimentation and ordinary curve fit examined by ZsimpWin simulation software as in **Fig. 7 (b)**. An inset of **Fig. 7 (b)** shows matched equivalent circuit for electrode CF2 have circuitry constraints viz charge transfer resistance Rs = 2.831 Ω, R_{CT} =

3.816 Ω, R_L = 1343 Ω, CPE= 3.062×10^{-5} F, CPE=1.130×10^{-3} F, and W= 3.622×10^{-4} F. **Fig. 7 (c)** displays the bode waveform for the CF2 electrode, drawn at OCP -0.7903 V for 5 mA in 1M KOH. The image itself recommends that as frequency grows, the phase angle progressively rises. Capacitive activity was most common at knee frequency. The phase angle keeps getting smaller as the frequency increases, indicating that resistive behavior was increasingly prevalent. At lower frequencies, materials behave capacitively, whereas at higher frequencies, they behave resistively [13] [15] . The Bode waveform for the CF2 electrode traced at OCP -0.7903 V for 5 mA in 1 M KOH was displayed in **Fig. 7 (d)**. The Bode plot, representing the variation in phase angle with frequency, was an effective tool for comprehending the typical electrode characteristic. The corresponding phase angle in the relatively low- frequency range, as shown in **Fig. 7 (d)**, was significantly close to 67.9°, indicating that the constructed electrode was approximately supercapacitive (90°) [16].

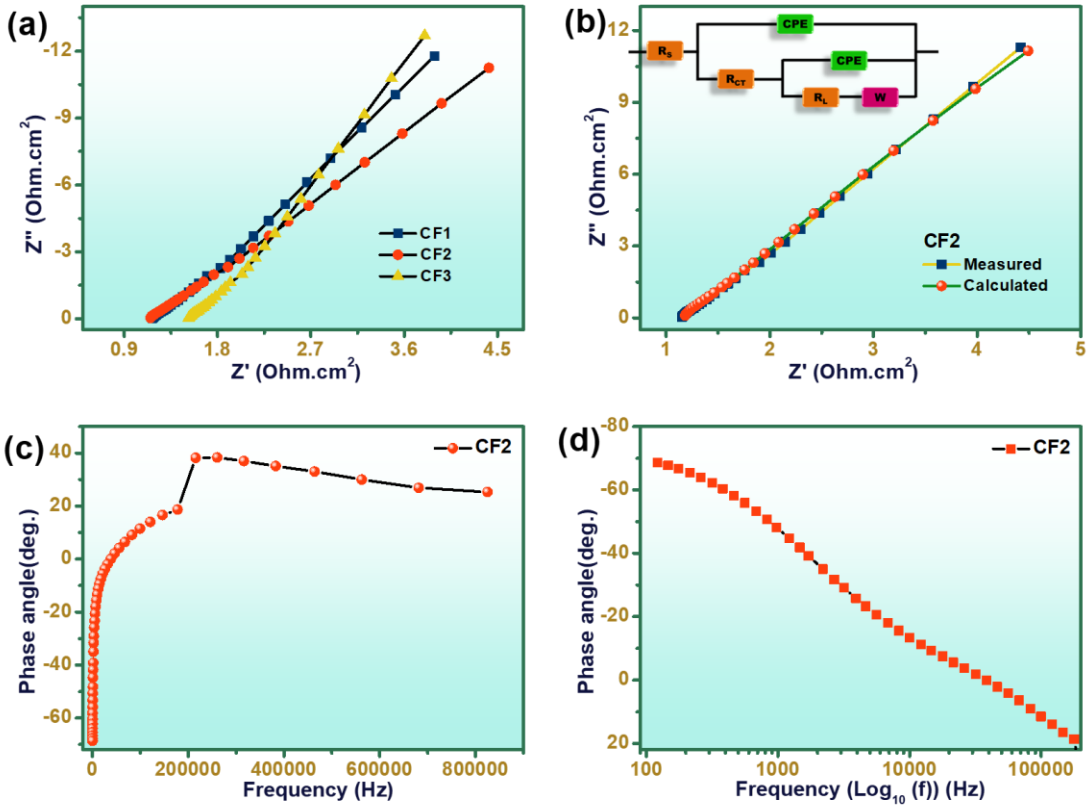

Fig. 7: EIS plot of sample electrode Fe_2O_3, **(a)** Nyquist plots of electrode CF1, CF2, and CF3, (b) nyquist plot & matched nyquist plot with marching circuit of electrode CF2, (c-d) bode plot of electrode CF2.

Conclusion

In this work, a successful coating of Fe_2O_3 nanomaterial was deposited on stainless steel (SS) working electrodes using the cost-effective and straightforward SILAR technique. The FE-SEM analysis revealed a grain-like morphology of the synthesized Fe_2O_3. The electrochemical performance of the developed electrode materials was notable, with a maximum specific capacitance (Cs) of 596 F/g at a scan rate of 5 mV/s in a 1M KOH electrolyte, positioning it favourably compared to other commonly used oxides. Furthermore,

the specific energy and specific power of the Fe2O3 electrodes were measured at 25.4 Wh/kg and 0.5 kW/kg, respectively. These findings underscore the potential of Fe_2O_3 as an electrically active material for high-performance supercapacitors, attributed to its exceptional electrochemical activity. This study demonstrates that Fe_2O_3, synthesized via the SILAR method, holds significant promise for future energy storage applications, offering both high efficiency and performance.

Institutional Review Board Statement: Not applicable.

Informed Consent Statement: Not applicable.

Data Availability Statement: Data will be made available on request

Conflicts of Interest

The authors declare that they have no known competing financial interests or personal relationships that could have appeared to influence the work reported in this paper.

References

[1] N. C. Maile *et al.*, "Capacitive property studies of inexpensive SILAR synthesized polyaniline thin films for supercapacitor application," *SN Appl. Sci.*, 2019, doi: 10.1007/s42452-019-1403-6.

[2] P. M. Kulal, D. P. Dubal, C. D. Lokhande, and V. J. Fulari, "Chemical synthesis of Fe2O3 thin films for supercapacitor application," *J. Alloys Compd.*, 2011, doi: 10.1016/j.jallcom.2010.11.091.

[3] S. S. Raut and B. R. Sankapal, "Comparative studies on MWCNTs, Fe2O3 and Fe2O3/MWCNTs thin films towards supercapacitor application," *New J. Chem.*, 2016, doi: 10.1039/c5nj03628c.

[4] S. Shivakumara, T. R. Penki, and N. Munichandraiah, "High specific surface area α-Fe2O3 nanostructures as high performance electrode material for supercapacitors," *Mater. Lett.*, 2014, doi: 10.1016/j.matlet.2014.05.160.

[5] G. Binitha *et al.*, "Electrospun α-Fe2O3 nanostructures for supercapacitor applications," *J. Mater. Chem. A*, 2013, doi: 10.1039/c3ta12352a.

[6] K. Xie *et al.*, "Highly ordered iron oxide nanotube arrays as electrodes for electrochemical energy storage," *Electrochem. commun.*, 2011, doi: 10.1016/j.elecom.2011.03.040.

[7] D. Sarkar, M. Mandal, and K. Mandal, "Design and synthesis of high performance multifunctional ultrathin hematite nanoribbons," *ACS Appl. Mater. Interfaces*, 2013, doi: 10.1021/am403762d.

[8] S. Chaudhari, D. Bhattacharjya, and J. S. Yu, "1-Dimensional porous α-Fe2O3 nanorods as high performance electrode material for supercapacitors," *RSC Adv.*, 2013, doi: 10.1039/c3ra44159h.

[9] R. G. Bobade *et al.*, "Concentration-dependent SILAR synthesized Di-bismuth copper oxide nano-materials electrode in asymmetric supercapacitor," *J. Mater. Sci. Mater. Electron.*, vol. 35, no. 2, p. 129, Jan. 2024, doi: 10.1007/s10854-023-11818-4.

[10] R. G. Bobade, N. B. Dabke, S. F. Shaikh, B. J. Lokhande, R. S. Mane, and R. C. Ambare, "Facile chemical synthesis of BaO:MgO nanorods for designing distinctive solid-state asymmetric supercapacitor device with activated carbon," *J. Energy Storage*, vol. 84, p. 110776, Apr. 2024, doi: 10.1016/j.est.2024.110776.

[11] C. Xia, C. Hu, Y. Xiong, and N. Wang, "Synthesis of α-Fe2O3 hexagons and their

magnetic properties," *J. Alloys Compd.*, 2009, doi: 10.1016/j.jallcom.2009.02.106.

[12] M. Aalim, I. Irshad, A. M. Tantray, A. Sohail, B. Want, and M. A. Shah, "Effect of chromium (Cr)-doping on electrochemical performance of microwave synthesized hematite (α-CrxFe2−xO3) nanosheets for supercapacitor application," *J. Mater. Sci. Mater. Electron.*, 2023, doi: 10.1007/s10854-023-10825-9.

[13] R. G. Bobade, U. T. Nakate, P. Roasiah, M. Ouladsmane, B. J. Lokhande, and R. C. Ambare, "Nanoarchitectonics of Bi2CuO4 electrodes for asymmetric Bi2CuO4//AC solid-state device in supercapacitor application," *Inorg. Chem. Commun.*, vol. 154, p. 110998, Aug. 2023, doi: 10.1016/j.inoche.2023.110998.

[14] R. G. Bobade *et al.*, "Influence of Deposition Potential on Electrodeposited Bismuth-Copper Oxide Electrodes for Asymmetric Supercapacitor," *Batter. Supercaps*, 2024, doi: 10.1002/batt.202400163.

[15] D. S. Gaikwad *et al.*, "SILAR-synthesized Co3O4/Bi2O3 on copper substrate nanocomposite electrode and asymmetric Co3O4/Bi2O3/CuO: AC solid-state device in supercapacitor," *J. Mater. Sci. Mater. Electron.*, 2024, doi: 10.1007/s10854-024-12220-4.

[16] B. Pandit *et al.*, "One-pot hydrothermal preparation of hierarchical manganese oxide nanorods for high-performance symmetric supercapacitors," *J. Energy Chem.*, vol. 65, pp. 116–126, Feb. 2022, doi: 10.1016/j.jechem.2021.05.028.